A bacterial glycan core linked to surface (S)-layer proteins modulates host immunity through Th17 suppression

Rajendra P. Settem[1], **Kiyonobu Honma**[1], **Takuma Nakajima**[1], **Chatchawal Phansopa**[2], **Sumita Roy**[2], **Graham P. Stafford**[2], and **Ashu Sharma**[1,*]

[1]Department of Oral Biology, School of Dental Medicine, University at Buffalo, State University of New York, Buffalo, NY 14214, USA

[2]Oral and Maxillofacial Pathology, School of Clinical Dentistry, Claremont Crescent, University of Sheffield, Sheffield S10 2TA, UK

Abstract

Tannerella forsythia is a pathogen implicated in periodontitis, an inflammatory disease of the tooth supporting tissues often leading to tooth loss. This key periodontal pathogen is decorated with a unique glycan core O-glycosidically linked to the bacterium's proteinacious surface(S)-layer lattice and other glycoproteins. Herein we show that the terminal motif of this glycan core acts to modulate dendritic cell effector functions to suppress Th17 responses. In contrast to the wild-type bacterial strain, infection with a mutant strain lacking the complete S-layer glycan core induced robust Th17 and reduced periodontal bone loss in mice. Our findings demonstrate that surface glycosylation of this pathogen acts to ensure its persistence in the host by suppressing Th17 responses. In addition our data suggest that the bacterium then induces the TLR2-Th2 inflammatory axis that has previously shown to cause bone destruction. Our study provides a biological basis for pathogenesis and opens opportunities in exploiting bacterial glycans as therapeutic targets against periodontitis and a range of other infectious diseases.

INTRODUCTION

Periodontitis is a chronic inflammatory disease whose pathology is defined by interplay between bacterial factors and host immune responses. *Tannerella forsythia* is a Gram-negative periodontal bacterium, which together with *Porphyromonas gingivalis* and the spirochete *Treponema denticola* constitutes the so-called 'red complex' consortium implicated in the etiology of periodontitis [1]. These bacteria inhabit subgingival biofilms in the human oral cavity where they modulate immune responses to instigate the periodontal tissue and bone destruction that is a hallmark of this disease. Furthermore, clinical studies also suggest a link between periodontitis and systemic diseases such as cardiovascular disease, diabetes and obesity [2, 3], and rheumatoid arthritis [4]. In some respects, the etiology of periodontitis is somewhat analogous to that of inflammatory bowl disease (IBD) where

[*]Correspondence: sharmaa@buffalo.edu Tel: (716) 829-2759; Fax: (716) 829-3942.

disturbances in host defense responses against gut flora contribute to the disease progression [5].

T. forsythia is a relatively under-studied pathogen despite being a key member of the pathogenic consortium. Its virulence mechanisms are just beginning to be revealed [6, 7]. In contrast to its red complex partners, *T. forsythia* lacks surface fimbriae, capsule and is non-motile but exclusively possesses a unique surface layer (S-layer) glycoprotein lattice. S-layers are water-insoluble proteins intrinsically capable of self-assembling into crystalline lattices on bacterial cell surfaces, and are believed to provide selective advantages to bacteria such as resistance to predation or immune clearance [8]. Interestingly, *T. forsythia* is the only Gram-negative bacterium that is known to possess a glycosylated S-layer [9]. It is composed of two high molecular weight glycoproteins, TfsA and TfsB, with predicted protein molecular masses of 135- and 154-kDa, respectively [9]. However, due to glycosylation, TfsA and TfsB proteins migrate as 200- and 210-kDa molecular size bands on SDS-PAGE, respectively [9]. We previously identified a genetic operon involved in the glycosylation of these S-layer proteins and predicted a direct role for the *wecC* gene (TF2055; postulated to encode UDP-N-acetylmannosaminuronic acid dehydrogenase) in the glycosylation of S-layer proteins, and showed that this plays a role in defining the physical properties of the cell surface affecting biofilm formation on inert surfaces [10]. In line with our hypothesis, a recent study identified that the *wecC* operon in *T. forsythia* plays a role in O-glycosylation of the S-layer glycoproteins with a unique oligosaccharide core [11]. Specifically, *wecC* seems to be key to the addition of a terminal sugar motif consisting of two sub-terminal mannosuronic acid residues and a terminal pseudaminic acid residue (Pse5Am7Gc, 5-acetimidol-7-N-glycolyl-pseudaminic acid) on this oligosaccharide core [11].

Cell surface glycosylation in bacteria can modulate immune responses during pathogenesis [12, 13]. In this regard, much of our knowledge on the role of glycosylation in bacteria colonizing the mucosal surfaces has come from the studies of capsule polysaccharides, glycosylated flagella/pilli and outer-membrane glycoproteins in gut dwelling organisms such as *Bacteroides fragilis* and S-layer from Gram positive bacteria. For example, evidence obtained from *Bacteroides* spp. indicate that surface polysaccharides can modulate dendritic cell activation and cytokine production [14, 15]. These immunomodulatory polysaccharides can regulate the differentiation of CD4(+) T cells and IL-10 secretion via Toll-like receptor 2 signaling [16]. Likewise, the Gram-positive *Lactobacillus acidophilus* S-layer glycoprotein can regulate dendritic cell (DC) function by interacting with the C-type lectin receptor DC-SIGN (dendritic cell-specific intercellular adhesion molecule-3-grabbing non-integrin) to induce specific T cell functions [17]. Similarly, *P. gingivalis* minor fimbriae glycoprotein targets DCs through DC-SIGN to elicit distinct effector functions [18, 19],

Recent *in vitro* studies suggested that *T. forsythia* S-layer proteinacious lattice per se could play a role in dampening the immune response during infection [20], However, the underlying mechanisms responsible for this immune suppression or the role of S-layer during periodontal inflammation in infection models has not been defined. Our hypothesis at the start of this study was that *T. forsythia* surface glycans would modulate DC and macrophage

responses, and influence T cell dependent periodontal inflammation and alveolar bone homeostasis.

Collectively, our results indicate that *Tannerella* surface glycosylation plays a role in restraining the Th17-mediated neutrophil infiltration in the gingival tissues. This probably allows the bacteria to persist and induce TLR2 and Th2 responses to cause tissue and bone destruction [21]. Overall, these results may help to explain how this oral pathogen utilizes its surface glycosylation to exploit the immune response to colonize and induce disease.

RESULTS

WecC controls surface protein glycosylation in *T. forsythia*

Our previous study showed that inactivation of the *wecC* gene in *T. forsythia* coding for a putative UDP-N-acetylmannosaminuronic acid dehydrogenase affects the surface glycosylation [10]. This was based on the findings that in comparison to the wild-type parental strain the *wecC*-deletion mutant showed increased surface hydrophobicity and the S-layer proteins of the deletion mutant migrated with increased mobility on SDS-PAGE gels [10]. A recent study by Posch and colleagues [11] which was published during the course of our study showed that this mutant lacks a terminal branch of the S-layer glycan. To phenotypically characterize the mutant further we performed ultrastructure analysis using transmission electron microscopy of ultra-thin sections of the wild-type *T. forsythia* and its *wecC* deletion mutant TFM-ED1 previously constructed in our laboratory [10] (hereafter called ED1). The results clearly demonstrate that while the wild-type cells show the characteristic ~ 25 nm thick regular lattice or striated 'teeth-like' S-layer first observed by Anne Tanner [22] (Fig. 1A, left), the ED1 mutant cells possess an irregular but intact S-layer of similar thickness (25nm)(Fig. 1A, right). This indicates that removal of the terminal glycosyl branches affects the S-layer assembly but not the secretion of localization on the cell surface. To further prove this notion we performed an outer membrane purification and observed both by SDS-PAGE glycoprotein-specific staining (Pro-Q Emerald) and western blotting using an anti-S-layer polyclonal antibody raised against intact purified wild-type S-layer, that the altered S-layer proteins are still present in the outer membrane fraction of ED1, albeit at an altered molecular weight (Fig. 1 A & B). In addition, and in agreement with Posch *et al* [11], we find that a number of other proteins appear to be glycosylated with a WecC-dependent glycosyl domain, but that the S-layer is the most abundant. In addition we also proved the surface localization of these glycoproteins using our antibody on *Tannerella* cells by fluorescence microscopy and showed that these proteins are localized on the periphery of the cell in both the wild-type and ED1 mutant (Fig. S1).

Additionally, since LPS and protein glycosylation are sometimes linked in Gram-negative bacteria, e.g. *Aeromonas* sp. [23], we examined whether the lipopolysaccharide pattern of the ED1 mutant was altered compared to the wild-type. Purified lipopolysaccharide fractions form the wild-type and the mutant strains were subjected to Urea-SDS-PAGE followed by LPS-silver staining [24]. The results (Fig. 1C) showed an identical electrophoretic pattern for the LPS of the two strains, indicating that the *wecC* deletion does not affect the chemical nature of LPS expression in *T. forsythia*. Taken together, these results imply that the ED1

mutant is defective with respect to surface glycosylation associated with the S-layer and other surface glycoproteins but does not present any abnormality with respect to LPS.

Glycosylation-deficient mutant induces increased NF-kB activity

We postulated that the wild-type and the ED1 strains would be differentially recognized by immune cells. This hypothesis was based on: i) pathogen-associated polysaccharides act as ligands for TLRs (TLR2 and TLR4), NODs and C-type lectin receptors; ii) surface glycosylation can modulate immune response by blocking recognition of other pathogen-associated molecules, and thus might help in immune evasion, and; iii) in a recent study a *T. forsythia* mutant completely deficient in S-layer was shown to cause increased secretion of inflammatory cytokines in a monocytic cell line and human gingival fibroblasts *in vitro* compared to the wild-type strain [20]. However, since the complete S-layer deletion strain was used in the previous study, it was not clear whether surface glycosylation *per se* was modulating any effects of the S-layer on the host response. Therefore, our ED1 mutant presents a unique opportunity to test the role of the novel protein glycosylation pattern of surface proteins in *Tannerella* on immune responses. Thus, we first investigated the inflammatory response to *T. forsythia* wild-type and ED1 mutant strains using a reporter cell line, THP-1-Blue that is derived from the human monocytic cell line THP-1. In addition this was stably transfected with a reporter plasmid expressing a secreted form of embryonic alkaline phosphatase (SEAP) under the control of an NF-κB- and AP-1-inducible promoter. The results showed significantly elevated SEAP activity in THP-1-Blue cells in response to ED1 challenge over THP-1-Blue cells challenged with the wild-type bacteria at a similar dose (Supplementary Fig. S2). These initial results provided a basis for dissecting the role of surface glycosylation in modulating the immune response to *T. forsythia* in detail.

Bacterial glycosylation regulates levels and nature of cytokine induction in APCs

As shown previously [21], *T. forsythia* challenge primarily induces Th2 development *in vivo*. We were therefore interested to investigate whether surface glycosylation in *T. forsythia* plays a role in modulating the secretion of specific T helper cell differentiating cytokines by antigen-presenting cells (APCs). For this purpose, mouse bone marrow-derived dendritic cells (mBMDCs) and macrophages were challenged with the *T. forsythia* wild-type or ED1 mutant cells at a multiplicity of infection (MOI) of 10. The cytokines secreted in the medium were then assayed by ELISA. BMDCs and peritoneal macrophages were purified by positive selection and confirmed to be 90-95% pure, verified by staining for CD11c, MHC-II, and CD86 (BMDCs) or CD11b (macrophages) by flow cytometry (data not shown). Pure *E. coli* LPS (eLPS) was used as a positive agonist. The data showed that *T. forsythia* ED1 mutant induced significantly higher amounts of IL-6 and IL-1β secretion in both BMDCs and macrophages compared to the wild-type *T. forsythia* (Fig. 2A). However, no significant difference was observed with regard to IL-10 secretion in either BMDCs or macrophages (Fig, 2A). As expected, eLPS induced potent production of these cytokines (Fig. 2A). Interestingly, IL-12p40 (the shared subunit for IL-12 and IL-23) and IL-23 levels were higher but IL-12p70 (IL-12 p35 and p40 heterodimer) level was lower in BMDCs challenged with the ED1 mutant compared to the wild-type strain. In macrophages, a similar pattern was observed for IL-12p40 and IL-23 (Fig. 2B). Strikingly, a heightened IL-12p40 response was observed in both DCs and macrophages. IL-12p40 can form a homodimer

(IL-12p80), which can potentially block Th1 differentiation through competing with IL-12 for IL-12R [25-27]. Moreover, IL-12p80 through its interaction with IL-12Rβ1 stimulates migration of DCs to chemokine CCL19 [28], and thus the heightened IL-12p40 dimer secretion in response to *T. forsythia* challenge might play a role in DC recruitment as well. As expected [21], no significant IL-12p70 secretion was observed in macrophages in response to ED1 challenge (Fig. 2B) or the wild-type bacteria (Fig. 2B). These results demonstrate that *T. forsythia* induces differential responses in APCs (BMDCs versus macrophages) with respect to the Th1 cytokine IL-12. This suggests that DCs and macrophages utilize a different mechanism to handle *T. forsythia*. While DCs and macrophages share many pattern-recognition receptors, differences in nucleosome remodeling for transcription and transcript stability in these cell types can impact the expression of cytokines. In support, *Mycobacterium tuberculosis* induces increased IL-12 secretion in DCs compared to that in macrophages through extensive nucleosome remodeling in DCs via the p40 promoter [29]. In addition, dendritic cell-specific intercellular adhesion molecule-3-grabbing non-integrin (DC-SIGN) lectin-like receptor can modulate the responses of other PRRs by moderating the crosstalk between intracellular signaling pathways [30, 31].

Surface glycosylation protects *T. forsythia* from DC recognition

The increased ability of the ED1 mutant to induce IL-23 secretion in BMDCs led us to hypothesize that glycosylation affects the ability of DCs to process the bacteria. To test this hypothesis, DCs were incubated with fluorescently-labeled bacteria at an m.o.i of 10 for 30 min and the ability of the DCs to bind/uptake bacteria was evaluated by flow cytometry. Flow cytometry analysis (Fig. 3 A & B) showed that a significantly lower population of DCs stained positive when incubated with the wild-type *T. forsythia* compared to ED1. Correspondingly, a larger DC population remained negative when incubated with wild-type *T. forsythia* cells compared to ED1 and *vice versa* (Fig. 3 A & B). There was an approximately two-fold increase in the mean fluorescent intensity of DCs (M2; Fig. 3C) associated with ED1 compared to the wild-type *T. forsythia* (Fig. 3C). Moreover, the flow cytometry data were confirmed by an in vitro bacterial killing assay in which bacteria were enumerated following incubation of live bacteria with DCs for different time points. The data from this assay show that a significantly greater numbers of ED1 cells than the wild-type strain associated with DCs initially (15 min; Fig 3 D). Moreover, the increased recognition of ED1 translated to an increased bacterial killing since a significantly fewer numbers ED1 cells were recovered at a later time point (60 min) compared to the wild-type strain (Fig. 3D). These results indicate that loss of surface glycosylation renders *T. forsythia* increasingly prone to capture by DCs, which probably leads to enhanced bacterial processing by DCs as well

Surface glycosylation deficiency results in reduced *in vivo* virulence

In vitro data above show that ED1 mutant is significantly more potent than the wild-type strain in causing IL-1β and IL-6 secretion in both DCs and macrophages. Since DCs are able to recognize the glycosylation-deficient ED1 mutant more efficiently and respond by secreting increased levels of IL-23, the contribution of surface glycosylation in modulating T helper cell responses and periodontal inflammation *in vivo* was determined. For this purpose, BALB/cJ mice were infected with 6 doses of bacteria (10^8 cfu per dose) at 48 h

intervals, using either the wild-type or ED1 mutant cells by oral gavage. Control sham-infected animals were inoculated with vehicle (1% carboxymethyl cellulose) alone. One week following the last infection, PCR analyses of oral swabs confirmed infection via expression *T. forsythia*-specific 641-bp 16s rDNA product for all mice infected with *T. forsythia* (wt) or ED1 mutant (n=8 per group). As expected, sham-infected mice were positive only for the 1.4 kb universal eubacteria 16s rDNA product but not *T. forsythia* specific 16s rDNA product (supplementary Fig. S3). Furthermore, analysis of *T. forsythia*-specific IgG titers 6 weeks after the first infection confirmed that the mice were successfully infected. Our results showed that the bacteria-specific serum IgG titers to the wild-type and ED1 strains increased several fold over sham-infected levels in mice infected with corresponding strains (Fig. 4A). The low IgG titer to *T. forsythia* even in the sham-infected mice is presumably due to non-specific cross reaction to anti-bacterial antibodies elicited to normal resident bacteria. Taken together the results of PCR analysis and antibody responses, indicated that mice orally gavaged with the *T. forsythia* wild-type and ED1 strains were successfully infected with each strain.

To assess periodontal bone loss induction, the distance from the alveolar bone crest (ACB) to the cementoenamal junction (CEJ) was measured at 14 buccal sites six weeks post-infection. As expected, significant alveolar bone loss was observed in *T. forsythia* wild-type infected mice at multiple sites compared to the sham-treated controls (Fig. 4 B & C). Strikingly, mice infected with the ED1 mutant did not show statistically significant periodontal bone loss. Moreover, the net alveolar bone loss induced by the ED1 mutant (calculated as the average total ABC-CEJ distance of the sham-treated group subtracted from the bacteria-infected group) was significantly lower than the net bone loss induced by the *T. forsythia* wild-type strain (Fig. 4C). Thus, the *T. forsythia* ED1 mutant is less virulent in a periodontitis model.

Resistance to glycosylation-deficient strain correlates with Th17 responses

We compared Th cell response of mice infected with the wild-type and the ED1 strains by analyzing T helper cells from draining cervical lymph nodes (cLN) of infected mice. Mice were infected orally 3 times at 48 h intervals with the wild-type or the ED1 strain, and 72 h after the last infection, cLN cells were stimulated with anti-CD3 and -CD28 Abs to stimulate the TCR and induce cytokine production. Cells were then treated with PMA-ionomycin, stained for cell surface CD4, and intracellularly stained for IL-5, IFN-γ and IL-17 to detect Th2, Th1 and Th17 cells, respectively. As shown (Fig. 5), in wild-type strain infected mice (susceptible to bone loss), the number of Th2 cells increased while the number of Th1 and Th17 cells decreased following infection (Fig. 5). Conversely, the number of Th2 cells was reduced with a concomitant increase in Th17 cells in mice infected with ED1 (resistant mice) compared to sham (Fig. 5). The number of Th1 cells decreased significantly in both the wild-type *T. forsythia* and ED1 infected groups compared to sham. This decrease was greater following wild-type *T. forsythia* infection compared to ED1 infection. Since the ED1 mutant caused skewing to a Th17 response, we conclude that *T. forsythia* surface glycosylation plays a role in dampening Th17 responses.

Resistance to glycosylation-deficient strain correlates with decreased osteoclastic activity and increased neutrophil infiltration

To evaluate osteoclastic activity, maxillary bones were stained for TRAP (tartrate resistance alkaline phosphatase, a marker of osteoclasts) positive cells. Approximately a two-fold increase in the numbers of TRAP^{+} cells was observed in the wild-type *T. forsythia*-infected maxillae compared to those of ED1 mutant or sham-infected mice (Fig. 6 A & B). Thus, induction of alveolar bone loss induced by wild-type *T. forsythia* correlated with increased osteoclastic activity in maxillary bones. Strikingly, the ED1 infection did not enhance osteoclastic activity, even though increased Th17 response was observed in ED1 infected mice (Fig. 5). Interestingly, contrary to the role of Th17 in bone destruction as seen in rheumatoid arthritis [32], Th17 cells are playing a protective role in infection induced bone loss in the context of the oral niche.

To evaluate inflammatory cells in the gingival space, maxillae were stained with anti-CD45 and anti-neutrophil specific marker antibody. The results indicated that *T. forsythia* wild-type and ED1 infection caused an increase in the CD45+ lymphocytic population in gingival tissues compared to the sham-infected tissues (Fig. 7). In line with the increased ability of the ED1 to induce inflammatory cytokines (Fig. S1 & Fig 2A), this mutant also caused increased infiltration of CD45^{+} lymphocytes in gingival tissues (Fig. 7). There was approximately a 3-fold increase in neutrophil numbers in ED1 infected mice over wild-type strain infected mice (Fig. 7 B). Not surprisingly, the increase in neutrophil numbers following ED1 infection parallels the increase in Th17 response in ED1 infected mice.

Glycosylation-deficient strain is cleared faster than the wild-type strain from gingival tissues

Reduced alveolar bone loss paralleling increased neutrophil infiltration in gingival tissues in glycosylation-deficient strain infected mice suggested that neutrophils might be playing a role in bacterial clearance. To evaluate this possibility, bacterial burdens were estimated in gingival tissues of mice following infection. Our results show that in comparison to the wild-type strain the survival of glycosylation deficient strain was significantly reduced in mice (Fig. 8), suggesting that neutrophils are likely playing protective role in the current infection setting.

DISCUSSION

In this study, we investigated the immunomodulatory effect of WecC-dependent O-linked protein glycosylation in *T. forsythia*. We observed increased secretion of Th17 differentiating cytokines IL-23 and IL-6 secretion in BMDCs and macrophages in response to the *T. forsythia* strain ED1 lacking the terminal sugar motif of a O-glycan core compared to the *T. forsythia* ATCC 43037 strain having the complete glycosylation repertoire. Moreover, as would be predicted based on these cytokine expression profiles, an increase in Th17 cells was detected in draining lymph nodes of mice orally infected with the glycosylation deficient mutant ED1 compared to the wild-type strain. Further, the glycosylation deficiency impaired the bacterium's ability to induce alveolar bone loss, which our evidence suggests is due to an increase in the Th17 response following infection

and a resultant increased neutrophil infiltration in the gingival tissues. Moreover, in line with an increase in neutrophil infiltration, reduced bacterial loads were found associated with mouse gingival tissues. Therefore, the major finding of our study is that *Tannerella* surface glycosylation associated with S-layer and other surface glycoproteins helps in inhibiting bacterial association with DCs and in restraining Th17 response to bacterial challenge in a murine model.

The *T. forsythia* ED1 mutant used in this study was previously generated by our group by a specific deletion of the *wecC* gene (TF2055) postulated to encode UDP-N-acetylmannosaminuronic acid dehydrogenase [10]. This mutation results in altered glycosylation of S-layer glycoproteins [10], specifically it causes deletion of a terminal trisaccharide motif that consists of a terminally located mannosaminuronic acid (ManpNAcA) and pseudaminic acid (Pse5Am7Gc) residue linked to another mannosaminuronic acid residue [11]. Importantly both our TEM and outer membrane purification experiments illustrate that the ED1 strain contains an intact, if altered, S-layer that still forms a protein coat around the cell surface but lacks full glycosylation resulting in altered immune system interactions. Moreover, there are no obvious changes in LPS presentation as judged by electrophoretic analysis of LPS preparations, thus indicating that the observed phenotype of the ED1 mutant with respect to its ability to modulate the immune response is due to the loss of surface glycosylation and not due to LPS abnormality.

In addition it is thought that the S-layer of *T. forsythia* is a member of a set of proteins in that are thought to be secreted by a novel protein secretion mechanism known as the c-terminal signal secreted proteins [33]. These are thought to be secreted via a largely uncharacterized protein secretion machinery that relies on a conserved c-terminal secretion domain (CTD) and has been most well-characterized in the partner periodontal pathogen *P. gingivalis* [34, 35]. In *P. gingivalis* it is becoming clear that the CTD acts as a recognition site for a sortase-like protease that cleaves the CTD sequence linking C-terminal carbonyl to a sugar amine of A-LPS [35]. Our finding that the altered S-layer (and other) glycoproteins of the ED1 strain can still be exported to the surface suggest that the glycosylation pattern of CTD proteins in *T. forsythia* is not likely to be part of the recognition signal for CTD system in *T. forsythia*.

Periodontitis is an inflammatory disease in which both innate and adaptive immune responses play critical roles. For instance, impairment in neutrophil and macrophage recruitment due to deficiencies in adhesion molecules increases *P. gingivalis*-induced alveolar bone destruction [36], and destructive roles for T and B cells in periodontal pathogenesis is well documented [37, 38]. Similar to other inflammatory diseases, a disruption of the proper balance between individual T helper subtypes (Th1, Th2 and Th17) contributes to the progression of periodontitis. The role of these different Th cell types and how bacterial factors promote or downregulate specific Th cell types and disrupt this balance is a major focus of many investigations [39-42]. With respect to *T. forsythia*, we have previously shown that *T. forsythia* infection causes a Th2 bias because of TLR2 activation, and that TLR2-Th2 inflammatory axis is primarily responsible for *T. forsythia*-induced alveolar bone loss [21]. In the present study we show that surface glycosylation of *Tannerella* specifically acts to prevent Th17 generation, allowing generation of TLR2-dependent Th2 bias

beneficial to bacteria by causing inflammatory tissue destruction and releasing components needed for bacterial growth. The protective role of Th17 against *T. forsythia*-induced alveolar bone loss in the periodontitis mouse model is in agreement with the findings of a previous study showing increased susceptibility of IL-17 receptor deficient mice to the fellow periodontal pathogen *P. gingivalis* [43]. However, Th17 responses have also been implicated in the progression of periodontitis [39, 44]. It is likely that Th17 (IL-17) responses have protective as well as destructive roles during periodontal disease depending on the disease phase and the pathogens involved. Th17 during early stages may provide antimicrobial immunity and have a role in controlling the disease. Moreover, the presence of Th17 cells may not always translate to excessive IL-17 production deleterious to the periodontal tissue. This has been recently demonstrated in a recent study investigating *P. gingivalis*-induced inflammatory bone loss in older mice in which neutrophils and gamma-delta T cells, but not Th17 cells, were found to be the major source of IL-17 in the gingival tissue [45].

The present study highlights the fundamental role of *T. forsythia* surface glycosylation in restraining the Th17 response, which otherwise might be detrimental to the pathogen by facilitating its clearance through neutrophils. Our model of events, which is outlined in Figure 9 envisages that *T. forsythia* engagement of TLR2 by surface ligands such as BspA and lipoproteins then skew the responses toward Th2, inducing alveolar bone loss. The exact mechanism by which surface layer glycans help to suppress Th17 response is unknown. However, it is likely that glycosylation, by blocking APC uptake of bacteria as shown in the present study, might minimize the interactions of bacterial ligands with intracellular pattern-recognition receptors (NODs, TLR9). Another possibility exists that surface glycans by interacting with C-type lectin receptors (CTLRs) skew the response towards Th2. In this regard DC-SIGN as well as cytoplasmic NOD-like receptors have been shown to control Th2 responses [46]. While TLR2 signaling plays a dominant role in DCs against *T. forsythia* as shown previously, O-glycan mediated signaling and its crosstalk with TLR2 impacts the net outcome of the DC-*Tannerella* interactions. This is because the differential expression of IL-12p40, IL-12p70, and IL-23 cytokines was lost when both TLR2 and O-glycan mediated signaling were abolished (i. e. *tlr2*$^{-/-}$ DCs stimulated with ED1, supplementary Fig. S4). Here, it is also tempting to speculate that the terminal trisaccharide lacking in the S-layer glycoproteins of the ED1 mutant, which contains pseudaminic acid (a modified form of siaic acid in bacteria) can putatively interact with Siglecs (sialic acid binding Ig-like lectins) receptors on immune cells. Siglecs can act both as positive and negative regulators of immune response [47]. The presence of pseudaminic acid is not unique to the *T. forsythia* S-layer with the flagellin molecule of a range of species containing versions of this sugar [23]. While its role in flagellar glycosylation is thought to be largely structural, the non-glycosylated *Pseudomonas aeruginosa* flagellin is less immunostimulatory in inducing an IL-8 response than the wild-type glycosylated form of flagellin [48]. As outlined above our data suggest control of Th17 responses as key to periodontal disease progression, and it is of note that several other types of infection by other pathogens and human dwelling bacteria also influence this arm of the immune system. For example, another oral organism *Candida albicans* dampens Th17 responses *in vivo* by secreting yet to be identified factors [49]. In addition, the polysaccharide antigens (PSA) of the gut organism *Bacteroides fragilis* account

for the suppression of Th17 responses critical for its persistence in the gut [50]. Taken together these, and our, data suggest that therapeutic modulation of Th17 immunity might be an attractive strategy for clinical intervention of a range of pathologies including periodontitis.

In summary, S-layer glycosylation in *T. forsythia* acts by selectively suppressing the specific Th17 and innate immune neutrophil responses. The evolution of this trait by *T. forsythia* presumably increases its persistence in the human cavity by acting as an immune evasion tactic. At the same time the organism exploits TLR2 mediated Th2 responses to its advantage in colonization of its primary environmental niche within periodontal pockets, which ultimately results in alveolar bone loss and expansion of this habitat. Overall, these results highlight how glycosylation of its surface layer proteins is part of a range of novel strategies that this persistent colonizer of the oral cavity utilizes to both cause periodontal disease but also survive in the body for many years and cause recurring bouts of this condition. These data have wide-ranging implications for the mechanisms used by persistent bacterial pathogens in immune manipulation, evasion and exploitation and reveal yet more of the intricacies of bacterial-host interactions that have evolved over time.

EXPERIMENTAL PROCEDURES

Bacterial strains and culture conditions

T. forsythia ATCC 43037 was grown in TF-broth (brain heart infusion media containing 5 μg/ml hemin, 0.5-μg/ml menadione, 0.001% N -acetylmuramic acid, 0.1% L-cysteine and 5% fetal bovine serum) as liquid cultures or on plates containing 1.5 % agar in broth under anaerobic conditions as described previously grown [51]. An isogenic *T. forsythia* mutant TFM-ED1 (hereafter called ED1) [10] inactivated of *wecC* gene encoding UDP-*N*-acetyl-mannosaminuronic dehydrogenase was grown in broth or agar plates containing 5 μg/mL erythromycin.

TEM method

For electron microscopy, 1ml of plate grown bacterial cell suspension of OD_{600} 1.0 was centrifuged and the supernatant was discarded. The cell pellet was washed twice with cacodylate buffer (0.1M cacodylate buffer pH 7.4) for 5 mins before fixing with 3% glutaraldehyde for 2-4h at 4 °C. This was then rinsed in cacodylate buffer (pH 7.4) 3×20 mins 4°C. The pellet was then soaked with 1% aqueous OsO_4 (Osmium tetraoxide) for 1h room temperature (RT) and washed three times (2mins) with dH_2O at RT, followed by two washes (3 mins) with 70% ethanol at RT, before two washes with 95% ethanol and two with 100%. After drying the pellet was then soaked twice for 15 minutes in Propylene oxide. This sample was then incubated overnight in propylene oxide:avaldite solution (1:1, v/v) for 16h (lids on) before removal and addition of 100% avaldite for 8h (lids off). The pellet was then embedded in fresh avaldite and left to polymerize at 60C for 24-48h. Avaldite was prepared using 20ml of Agar 100 epoxy resin, 16ml of hardener (DDSA), 8ml of hardener (MNA) and 1.3 ml of accelerator (BDMA, C.3%). The embedded cell pellet was sectioned at 70-90nm and placed on to a formvar-coated grid.

The grids were stained using uranyl acetate and lead citrate. Uranyl acetate (7%) was saturated in 50 % methanol and used for staining. Lead citrate was prepared by adding 1.33g lead nitrate, 1.76g sodium citrate in 50ml H_2O/NaOH. Stained cross sections were viewed by TEM at the University of Sheffield Electron Microscopy service in the Department of Biological Sciences.

Outer-membrane purification and analysis

Cells were incubated at 37 °C in an anaerobic atmosphere (10% CO_2, 10% H_2 and 80% N_2) for 3 days, harvested using sterile loops and resuspended by pipetting in 1 mL pre-chilled 50 mM HEPES, 50 mM NaCl, pH 7.4. Cell suspensions were placed in ethanol/ice water bath and lysed by sonication. Undisrupted cells and cell debris were pelleted by centrifugation at 15,000 rpm for 30 minutes at 4 °C and discarded. The supernatants were ultracentrifuged at 60,000 rpm in a Beckman Ti70.1 fixed angle rotor for 2 hours at 4 °C to pellet the inner and outer membranes. The supernatants were carefully decanted and discarded, while the membrane pellets were gently washed twice in 50 mM HEPES, 50 mM NaCl, pH 7.4. The pellets were then resuspended in 1 mL 50 mM HEPES, 50 mM NaCl, pH 7.4. To solubilize the inner membrane, an equal volume of 2% ($^v/_v$) sodium *N*-lauroyl sarcosinate in 50 mM HEPES, 50 mM NaCl, pH 7.4, was added and mixed thoroughly by pipetting, followed by an incubation at 37 °C for 30 minutes. The suspensions were centrifuged at 20,000 rpm for 30 minutes at 4 °C, and the supernatants containing the inner membrane fraction were carefully decanted. The outer membrane pellets were gently washed twice in 50 mM HEPES, 50 mM NaCl, pH 7.4, after which these pellets were resuspended in 500 μL 50 mM HEPES, 50 mM NaCl, pH 7.4, and stored at −20 °C.

Samples were then analysed by SDS-PAGE on Invitrogen NuPAGE 4-8% gradient gels and silver stained (BioRad SilverStainPlus). In addition parallel gels were oxidized with Periodic Acid before staining with a ProQ-Emerald glycoprotein staining kit from Molecular Probes according to manufacturer's instructions (visualized on a UV transilluminator). Samples were also transferred to Nitrocellulose membrane before probing with a rabbit antibody raised against purified intact S-layer and detected with anti-rabbit HRP and Pierce Supersignal WestPico chemiluminescent substrate before exposure to Kodak X-ray film and development in a Kodak X-Omat developer.

Production of anti S-layer antibody

Intact native S-layer from the wild-type *T. forsythia* 43037 was purified by cesium chloride gradient ultracentrifugation according to a previously described protocol [9] and 100 mg used to prepare antibodies in rabbits within the Sheffield Antibody unit (Bioserv UK Ltd).

LPS

Lipopolysaccharide was extracted from agar grown *T. forsythia* wild-type and ED1 strains using the equivalent of 1ml of an OD600 of 5 cells resuspended in PBS and using an LPS extraction kit from ChemBio with modifications. Briefly, after extraction the LPS was treated with Proteinase K and DNAse before re-extraction using the same kit according to manufacturer's instructions. LPS was visualized after separation of samples on a 10% Urea-

SDS-PAGE gel and oxidation with periodic acid (0.7%) before silver staining as described previously [24]

Inoculation of mice

Specific-pathogen-free BALB/cJ mice (Jackson Laboratory, Bar Harbor, ME, USA), 5-6 weeks old (8-10 female mice per group) at the start of the experiment were maintained in the Laboratory Animal Facility of the University at Buffalo. The Institutional Animal Care and Use Committee approved all the experimental protocols used in the study. After 1-week quarantine, mice were infected with *T. forsythia* as per previously described protocol [21]. After one week of Kanamycin (1 mg/mL) in drinking water *ad libitum* followed by a three-day antibiotic-free period to suppress the resident bacteria, mice were infected by oral gavage with 10^9 cfu /mL of live bacteria (*T. forsythia* wild-type ATCC 43037, or the mutant strain ED1) in 100 μL of PBS with 100 μl of 2% carboxymethyl cellulose (CMC) 3 times per week with 48-hour intervals and the schedule was repeated the following week. Control (sham-infected) mice received antibiotic pre-treatment and the 200μL of 1% CMC without the bacteria.

Assessment of infection by PCR

Sub gingival plaque samples were obtained from the molars of each mouse by placing sterile paper points (Johnson & Johnson, Piscataway, NJ, USA) sub-gingivally for 5 sec and then transferring and vortexing into 1 mL *T. forsythia* growth medium. Following one week's incubation, medium was spun at $12,000 \times g$ for 10 min, and the total bacterial genomic DNA was isolated with use of the Pure Gene genomic DNA isolation kit (Gentra, Minneapolis, MN, USA). PCR was performed on 250 ng of genomic DNA using a primer pair specific for *T. forsythia* 16S RNA gene (amplicon length 641 bp) or a universal primer pair that matches almost all bacterial 16S RNA genes (amplicon length 1.4 kb) as described previously [52]. PCR products were analyzed by agarose (1%) gel electrophoresis and ethidium bromide staining.

Assessment of alveolar bone loss

Horizontal bone loss around the maxillary molars was assessed by a morphometric method. After 6 weeks of first infection the mice were scarified and the serum samples were collected for IgG antibody response against the *T. forsythia* wild-type and ED1 strains by ELISA as described earlier [21]. Skulls were autoclaved, de fleshed and jaws were immersed in 3 percent hydrogen peroxide overnight and stained with 1 % methylene blue. The distances between the alveolar bone crest (ABC) and cement-enamel junction (CEJ) considered as alveolar bone loss were measured by two independent evaluators in blinded fashion at 7 buccal sites on each side with the help of a dissecting microscope attached to an imaging system with a software (Aquinto imaging system, a4i America, Brook-Anco, Rochester, NY).

Real-time PCR quantification of bacterial burden

Maxillary periodontal tissues (soft gingival and hard tissue) were excised on day 10 postinfection from mice. DNA was extracted using a DNeasy tissue kit (Qiagen, Valencia,

CA), and *Tannerella forsythia* loads were determined by real-time PCR with primers targeting 16S rRNA gene described above using an iCycler IQ and SYBR green master mix from Bio-Rad (Hercules, CA), In addition, mouse glyceraldehyde-3-phosphate dehydrogenase (*gapdh*) gene amplified (primers 5′-GCACAGTCAAGGCCGAGAAT-3′ and 5′-GCCTTCTCCATGGTGGTGAA-3′) from the same sample was used to normalize bacterial loads in extracted tissues as described [53]; bacterial loads were expressed as the number of Log_{10} CFUs per 10^9 copies of *gapdh*. The real-time Ct values were converted to weights of DNA by interpolation from DNA weight versus Ct standard curve. For calculating CFUs from the weights of DNA, the genome size of 3.4 MB for *T. forsythia* (http://www.homd.org) was used.

T. forsythia specific IgG antibody response by ELISA

T. forsythia wild-type and ED1 strain specific IgG antibody responses were measured by ELISA as described previously [21]. Briefly, 96-well Immuno-Maxisorp plates (Nalgene Nunc International, Rochester, NY) coated with formalin-fixed bacteria (10^9 cells/mL and 100μL/well) were incubated with serial dilutions of mouse sera, followed by HRP-conjugated goat anti-mouse IgG (Bethyl Laboratories, TX). ELISA wells were color developed with TMB Microwell enzyme substrate (Kirkgaards and Perry, MD) and plates were read at 495 nm. Titers was defined as the log2 of the highest dilution with a signal that was 0.1 optical density unit above the background level.

Generation of bone marrow derived dendritic cells and *in vitro* stimulation

Immature DCs were generated by using EasySep mouse CD11c positive selection kit (Stem cell technologies, USA) following the manufactures instructions. Briefly bone marrow progenitor cells were flushed with a 23 gauge needle in to the recommended medium. Disperse the clumps by gently passing the cell suspension through syringe and remove the debris by passing cell suspension through 70μm nylon cell strainer. After centrifugation resuspend in RPMI 1640 which contains 10 percent heat inactivated fetal calf serum (FCS), 2 mM glutamine, penicillin and streptomycin, 5 μM 2-mercatoethanol and GM-CSF(10 ng/mL). Plate 20 mL/150 mm Petri dish and incubate at 37°C for 5 days. Collect non-adherent cells, wash once and purify the CD11c positive cells by using purple Easy Sep magnet (Stem cell technologies). This protocol yielded BMDCs with > 93% purity. Purified bone marrow derived dendritic cells (BMDCs) were stimulated with bacteria for 12 h and the cytokine levels in the medium were quantified by ELISA.

For DC-mediated bacterial processing, BMDCs were infected with live bacteria at MOI of 1:10 in antibiotic free medium and at time points 15 and 60 minute post infection BMDC were extensively washed, lysed with sterile water, serially diluted and bacterial CFU determined by plating.

Isolation of peritoneal macrophages and challenge with stimulants

Mouse peritoneal macrophages were prepared as described previously [54] Purified macrophages were seeded in 48-well culture plates at a density of 10^5 cells per well in 250μl growth medium. *T. forsythia* cells were enumerated with Petroff-Hausser chamber immediately prior to each experiment. For challenge, multiplicity of infection (m.o.i;

number of bacteria per mammalian cell) of 10 was used. *E. coli* LPS (100ng/mL) was used as a positive control. After 12 hrs of stimulation cytokine levels were quantified by ELISA.

Determination of cytokine levels by ELISA

Culture supernatants were collected from BMDCs pulsed with TF strains (TF 43037, TFM-ED1-*Wec C* mutant) to assess the levels of IL-1β, IL-6, IL-12p40, IL-12p70, IL-23 and IL-10 by ELISA with Ready-SET-Go kits (eBioscience, San Diego, CA, USA) as per manufacturer instructions. Supernatants were used as undiluted and 1:10 fold dilutions. The detection limit for all cytokines was 5 pg /mL.

Intracellular staining and FACS analysis

The following Abs and isotype controls were purchased from eBiosciences: PE-conjugated anti–IFN-γ, IL-5 and rat IgG2a; PECy5-labeled anti-CD4; anti-CD80 (16-10A**1**) and anti-CD83 (Michel-17); PE-conjugated anti-CD11c (N418); hamster IgG, and; PE-conjugated anti-IL-17A (eBio17B7). For intracellular staining, cell suspensions from cervical lymph nodes (cLNs) were stimulated with anti-CD3 and anti-CD28 Abs (eBioscience) for 48 h, followed by PMA (50 ng/ml), ionomycin (1 μg/ml), and brefeldin A (10 μg/ml) for 6 h. Cells were washed, incubated with FcR block (1 μg/ml; eBiosciences), and stained for CD4. Cells were fixed with 2% paraformaldehyde, permeabilized with 0.1% saponin (Sigma), and stained for IL-5, IL-17, or IFN-γ. Cells were analyzed on a FACS Calibur (BD Biosciences) with FCS Express software (DeNovo Software).

Quantification of CD45+ cells and infiltrated neutrophils

The right and left halves of the maxillary and mandibular bones were removed, fixed and embedded in paraffin; 4-μm sections were cut and mounted. They were deparafinized in xylene and hydrated in graded ethanol. After antigen retrieval by incubating at 90 °C for 10 min with BD Retrievagen A (BD PharMingen), specimens were sequentially incubated in: (i) blocking solution containing and 0.1% Triton X-100 in 0.1 M PBS for 1 h at room temperature; (ii) monoclonal rat anti-mouse CD45 (BD PharMingen) antibody diluted 1:30 in PBS containing 0.1% Triton X-100 or anti-neutrophil marker antibody (NIMP-R14, Santacruz Biotechnology, CA,USA) for 1 h at room temperature. The slides were incubated with a biotinylated secondary antibody (goat anti-rat) followed by an avidin-biotin complex developed with 3, 3-diaminobenzidine (DAB) (Vector Labs, Burlingame, CA); the counter stain was haematoxylin. After each step, slides were rinsed in PBST (3 × 10 min). Slides were scanned at an absolute magnification of 400X at using the Aperio Scan Scope CS system (Aperio Technologies, Vista CA). Slides (six slides per mouse) were viewed and analyzed remotely using desktop personal computers employing the virtual image viewer software (Aperio). Antibody positive cells (stained brown) were enumerated manually in the inter-dental areas from the first to third molar at randomly selected locations in each slide (6 per slide). The areas associated with these locations were then obtained from the software to calculate the average cell densities per square millimeter.

TRAP staining

Mice maxillary and mandibular bones ($n = 4$) were fixed in 10% phosphate-buffered formalin and decalcified in 10% EDTA. The samples were then embedded in paraffin, and sections at 4 μm were prepared and stained for tartrate-resistant acid phosphatase (TRAP; Sigma).The TRAP-stained whole slides were digitally scanned immediately with a Scan Scope CS system (Aperio) to minimize color fading. The scanned slides were viewed with Image Scope viewing software (Aperio). The right maxillary and mandibular inter dental areas (average of 10 higher power fields/ slide) of the crestal alveolar bone from the first molar to third molar were used to quantify osteoclasts.

Data analysis

Data were analyzed on Graph Pad Prism software (Graph Pad, San Diego, CA). Comparisons between groups were made using a Student's *t* test (between two groups) Or ANOVA (multiple group comparisons), as 1 appropriate. Statistical significance was defined as $p < 0.05$.

Supplementary Material

Refer to Web version on PubMed Central for supplementary material.

Acknowledgments

REFERENCES

1. Socransky SS, Haffajee AD, Cugini MA, Smith C, Kent RL Jr. Microbial complexes in subgingival plaque. J. Clin. Periodontol. 1998; 25:134–144. [PubMed: 9495612]

2. Seymour GJ, Ford PJ, Cullinan MP, Leishman S, Yamazaki K. Relationship between periodontal infections and systemic disease. Clin Microbiol Infect. 2007; 13(Suppl 4):3–10. [PubMed: 17716290]

3. Pischon N, et al. Obesity, Inflammation, and Periodontal Disease. J. Dent. Res. 2007; 86:400–409. [PubMed: 17452558]

4. Moen K, et al. Synovial inflammation in active rheumatoid arthritis and psoriatic arthritis facilitates trapping of a variety of oral bacterial DNAs. Clin. Exp. Rheumatol. 2006; 24:656–663. [PubMed: 17207381]

5. Xavier RJ, Podolsky DK. Unravelling the pathogenesis of inflammatory bowel disease. Nature. 2007; 448:427–434. [PubMed: 17653185]

6. Sharma A. Virulence mechanisms of *Tannerella forsythia*. Periodontol 2000. 2010; 54:106–116. [PubMed: 20712636]

7. Stafford G, Roy S, Honma K, Sharma A. Sialic acid, periodontal pathogens and *Tannerella forsythia*: stick around and enjoy the feast! Mol Oral Microbiol. 2012; 27:11–22. [PubMed: 22230462]

8. Sara M, Sleytr UB. S-Layer proteins. J. Bacteriol. 2000; 182:859–868. [PubMed: 10648507]

9. Lee SW, et al. Identification and characterization of the genes encoding a unique surface (S-) layer of *Tannerella forsythia*. Gene. 2006; 371:102–111. [PubMed: 16488557]

10. Honma K, Inagaki S, Okuda K, Kuramitsu HK, Sharma A. Role of a *Tannerella forsythia* exopolysaccharide synthesis operon in biofilm development. Microb. Pathog. 2007; 42:156–166. [PubMed: 17363213]

11. Posch G, et al. Characterization and scope of S-layer protein O-glycosylation in *Tannerella forsythia*. J. Biol. Chem. 2011

12. Lebeer S, Vanderleyden J, De Keersmaecker SC. Host interactions of probiotic bacterial surface molecules: comparison with commensals and pathogens. Nat. Rev. Microbiol. 2010; 8:171–184. [PubMed: 20157338]

13. Szymanski CM, Wren BW. Protein glycosylation in bacterial mucosal pathogens. Nat. Rev. Microbiol. 2005; 3:225–237. [PubMed: 15738950]

14. Eynon EE, Zenewicz LA, Flavell RA. Sugar-Coated Regulation of T Cells. Cell. 2005; 122:2–4. [PubMed: 16009124]

15. Mazmanian SK, Liu CH, Tzianabos AO, Kasper DL. An Immunomodulatory Molecule of Symbiotic Bacteria Directs Maturation of the Host Immune System. Cell. 2005; 122:107–118. [PubMed: 16009137]

16. Round JL, Mazmanian SK. Inducible Foxp3+ regulatory T-cell development by a commensal bacterium of the intestinal microbiota. Proc. Natl. Acad. Sci. U. S. A. 2010; 107:12204–11209. [PubMed: 20566854]

17. Konstantinov SR, et al. S layer protein A of Lactobacillus acidophilus NCFM regulates immature dendritic cell and T cell functions. Proc. Natl. Acad. Sci. U. S. A. 2008; 105:19474–19479. [PubMed: 19047644]

18. Zeituni AE, Jotwani R, Carrion J, Cutler CW. Targeting of DC-SIGN on human dendritic cells by minor fimbriated *Porphyromonas gingivalis* strains elicits a distinct effector T cell response. J. Immunol. 2009; 183:5694–5704. [PubMed: 19828628]

19. Zeituni AE, McCaig W, Scisci E, Thanassi DG, Cutler CW. The native 67-kilodalton minor fimbria of *Porphyromonas gingivalis* is a novel glycoprotein with DC-SIGN-targeting motifs. J. Bacteriol. 2010; 192:4103–4110. [PubMed: 20562309]

20. Sekot G, et al. Potential of the *Tannerella forsythia* S-layer to delay the immune response. J. Dent. Res. 2011; 90:109–114. [PubMed: 20929722]

21. Myneni SR, et al. TLR2 signaling and Th2 responses drive *Tannerella forsythia*-induced periodontal bone loss. J. Immunol. 2011; 187:501–509. [PubMed: 21632710]

22. Tanner ACR, Listgarten MA, Ebersole JL, Strzempko MN. *Bacteroides forsythus* sp. nov., a slow growing, fusiform *Bacteroides* sp. from the human oral cavity. Int. J. Syst. Bacteriol. 1986; 36:213–221.

23. Tabei SM, et al. An *Aeromonas caviae* genomic island is required for both O-antigen lipopolysaccharide biosynthesis and flagellin glycosylation. J. Bacteriol. 2009; 191:2851–2863. [PubMed: 19218387]

24. Stafford GP, Hughes C. *Salmonella typhimurium* flhE, a conserved flagellar regulon gene required for swarming. Microbiology. 2007; 153:541–547. [PubMed: 17259626]

25. Holscher C. The power of combinatorial immunology: IL-12 and IL-12-related dimeric cytokines in infectious diseases. Med Microbiol Immunol. 2004; 193:1–17. [PubMed: 12836019]

26. Nigg AP, et al. Dendritic cell-derived IL-12p40 homodimer contributes to susceptibility in cutaneous leishmaniasis in BALB/c mice. J. Immunol. 2007; 178:7251–7258. [PubMed: 17513774]

27. Piccotti JR, Chan SY, Li K, Eichwald EJ, Bishop DK. Differential effects of IL-12 receptor blockade with IL-12 p40 homodimer on the induction of CD4+ and CD8+ IFN-gamma-producing cells. The Journal of Immunology. 1997; 158:643–648. [PubMed: 8992979]

28. Slight SR, Lin Y, Messmer M, Khader SA. Francisella tularensis LVS-induced Interleukin-12 p40 cytokine production mediates dendritic cell migration through IL-12 Receptor beta1. Cytokine. 2011; 55:372–379. [PubMed: 21669537]

29. Pompei L, et al. Disparity in IL-12 release in dendritic cells and macrophages in response to *Mycobacterium tuberculosis* is due to use of distinct TLRs. J. Immunol. 2007; 178:5192–5199. [PubMed: 17404302]

30. Geijtenbeek TB, Gringhuis SI. Signalling through C-type lectin receptors: shaping immune responses. Nat Rev Immunol. 2009; 9:465–479. [PubMed: 19521399]

31. Hovius JW, et al. Salp15 binding to DC-SIGN inhibits cytokine expression by impairing both nucleosome remodeling and mRNA stabilization. PLoS Pathog. 2008; 4:e31. [PubMed: 18282094]

32. Onishi RM, Gaffen SL. Interleukin-17 and its target genes: mechanisms of interleukin-17 function in disease. Immunology. 2010; 129:311–321. [PubMed: 20409152]

33. Veith PD, et al. Outer Membrane Proteome and Antigens of *Tannerella forsythia*. J Proteome Res. 2009; 8:4279–4292. [PubMed: 19663511]

34. Seers CA, et al. The RgpB C-terminal domain has a role in attachment of RgpB to the outer membrane and belongs to a novel C-terminal-domain family found in *Porphyromonas gingivalis*. J. Bacteriol. 2006; 188:6376–6686. [PubMed: 16923905]

35. Slakeski N, et al. C-terminal domain residues important for secretion and attachment of RgpB in *Porphyromonas gingivalis*. J. Bacteriol. 2011; 193:132–142. [PubMed: 20971915]

36. Baker PJ, DuFour L, Dixon M, Roopenian DC. Adhesion molecule deficiencies increase *Porphyromonas gingivalis*-induced alveolar bone loss in mice. Infect. Immun. 2000; 68:3103–3107. [PubMed: 10816450]

37. Baker PJ. The role of immune responses in bone loss during periodontal disease. Microbes Infect. 2000; 2:1181–1192. [PubMed: 11008108]

38. Baker PJ, Evans RT, Roopenian DC. Oral infection with *Porphyromonas gingivalis* and induced alveolar bone loss in immunocompetent and severe combined immunodeficient mice. Arch. Oral Biol. 1994; 39:1035–1040. [PubMed: 7717884]

39. Gaffen SL, Hajishengallis G. A new inflammatory cytokine on the block: re-thinking periodontal disease and the Th1/Th2 paradigm in the context of Th17 cells and IL-17. J. Dent. Res. 2008; 87:817–828. [PubMed: 18719207]

40. Gemmell E, Yamazaki K, Seymour GJ. Destructive periodontitis lesions are determined by the nature of the lymphocytic response. Crit. Rev. Oral Biol. Med. 2002; 13:17–34. [PubMed: 12097235]

41. Teng YT. Protective and Destructive Immunity in the Periodontium: Part 1--Innate and Humoral Immunity and the Periodontium. J. Dent. Res. 2006; 85:198–208. [PubMed: 16498065]

42. Teng YT. Protective and Destructive Immunity in the Periodontium: Part 2--T-cell-mediated Immunity in the Periodontium. J. Dent. Res. 2006; 85:209–219. [PubMed: 16498066]

43. Yu JJ, et al. An essential role for IL-17 in preventing pathogen-initiated bone destruction: recruitment of neutrophils to inflamed bone requires IL-17 receptor-dependent signals. Blood. 2007; 109:3794–3802. [PubMed: 17202320]

44. Ohyama H, et al. The involvement of IL-23 and the Th17 pathway in periodontitis. J. Dent. Res. 2009; 88:633–638. [PubMed: 19605880]

45. Eskan MA, et al. The leukocyte integrin antagonist Del-1 inhibits IL-17-mediated inflammatory bone loss. Nature immunology. 2012; 13:465–473. [PubMed: 22447028]

46. Pulendran B, Tang H, Manicassamy S. Programming dendritic cells to induce T(H)2 and tolerogenic responses. Nat. Immunol. 2010; 11:647–655. [PubMed: 20644570]

47. Crocker PR, Redelinghuys P. Siglecs as positive and negative regulators of the immune system. Biochem. Soc. Trans. 2008; 36:1467–1471. [PubMed: 19021577]

48. Verma A, Arora SK, Kuravi SK, Ramphal R. Roles of specific amino acids in the N terminus of *Pseudomonas aeruginosa* flagellin and of flagellin glycosylation in the innate immune response. Infect. Immun. 2005; 73:8237–8246. [PubMed: 16299320]

49. Cheng SC, et al. *Candida albicans* dampens host defense by downregulating IL-17 production. J. Immunol. 2010; 185:2450–2457. [PubMed: 20624941]

50. Round JL, et al. The Toll-like receptor 2 pathway establishes colonization by a commensal of the human microbiota. Science. 2011; 332:974–977. [PubMed: 21512004]

51. Sharma A, et al. Cloning, expression, and sequencing of a cell surface antigen containing a leucine-rich repeat motif from *Bacteroides forsythus* ATCC 43037. Infect. Immun. 1998; 66:5703–5710. [PubMed: 9826345]

52. Sharma A, et al. *Tannerella forsythia*-induced alveolar bone loss in mice involves leucine-rich-repeat BspA protein. J. Dent. Res. 2005; 84:462–467. [PubMed: 15840784]

53. Fang R, Ismail N, Shelite T, Walker DH. CD4+ CD25+ Foxp3-T-regulatory cells produce both gamma interferon and interleukin-10 during acute severe murine spotted fever rickettsiosis. Infect. Immun. 2009; 77:3838–3849. [PubMed: 19564386]

54. Zheng X, Goncalves R, Mosser DM. The Isolation and Characterization of Murine Macrophages. Curr. Protoc. Immunol. 2008; Chapter 14:Unit 14.1.
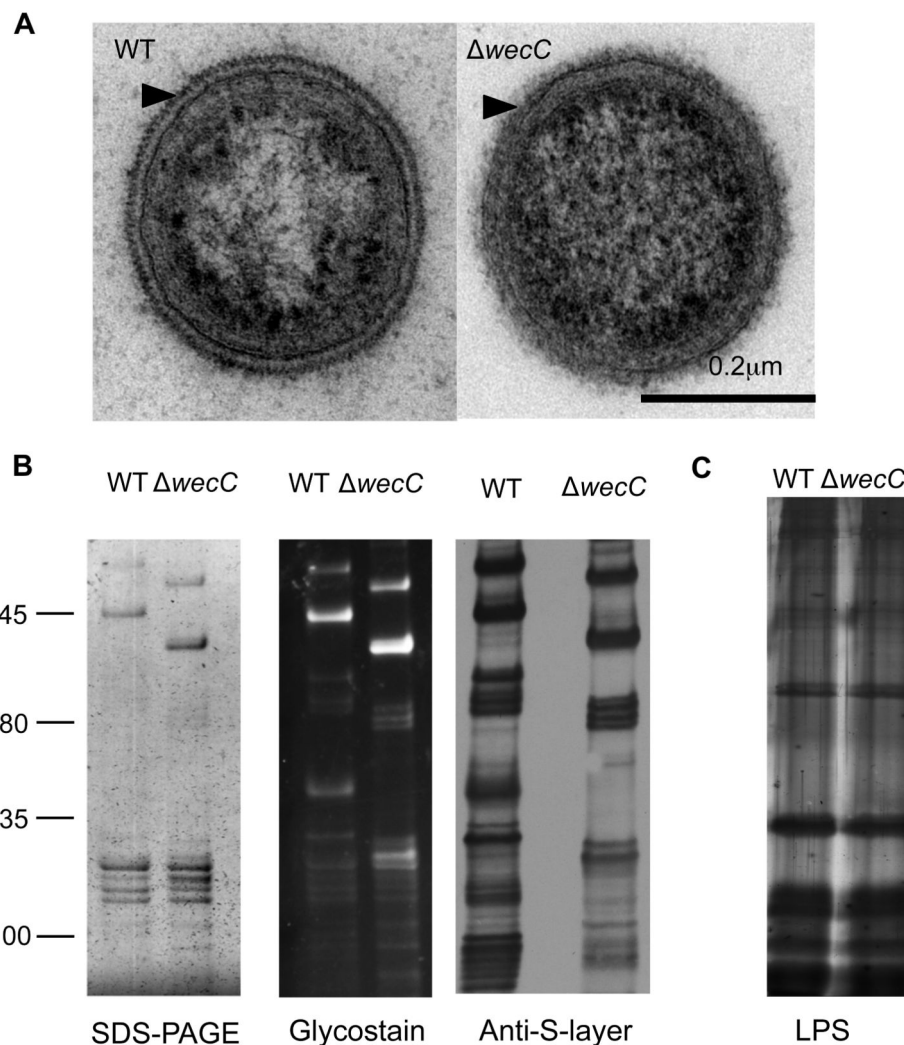
Fig. 1. Alteration of the glycosylation pattern of surface proteins of *T. forsythia* by deletion of the *wecC* gene results in an altered but intact S-layer and no changes in LPS

(A) TEM of negatively stained ultrathin sections of wild-type and ED1 mutant strains.
Arrowheads indicate the S-layer structure covering the outer membrane.

(B) Outer membrane preparations of wild-type and ED1 strains were separated on SDS-PAGE (4-8%) gels and stained with silver (left), ProQ Emerald glycostain (middle) and probed with an anti-S-layer antibody after western blotting (right)

(C) LPS was extracted and separated on a 10% Urea SDS-PAGE gel and silver stained
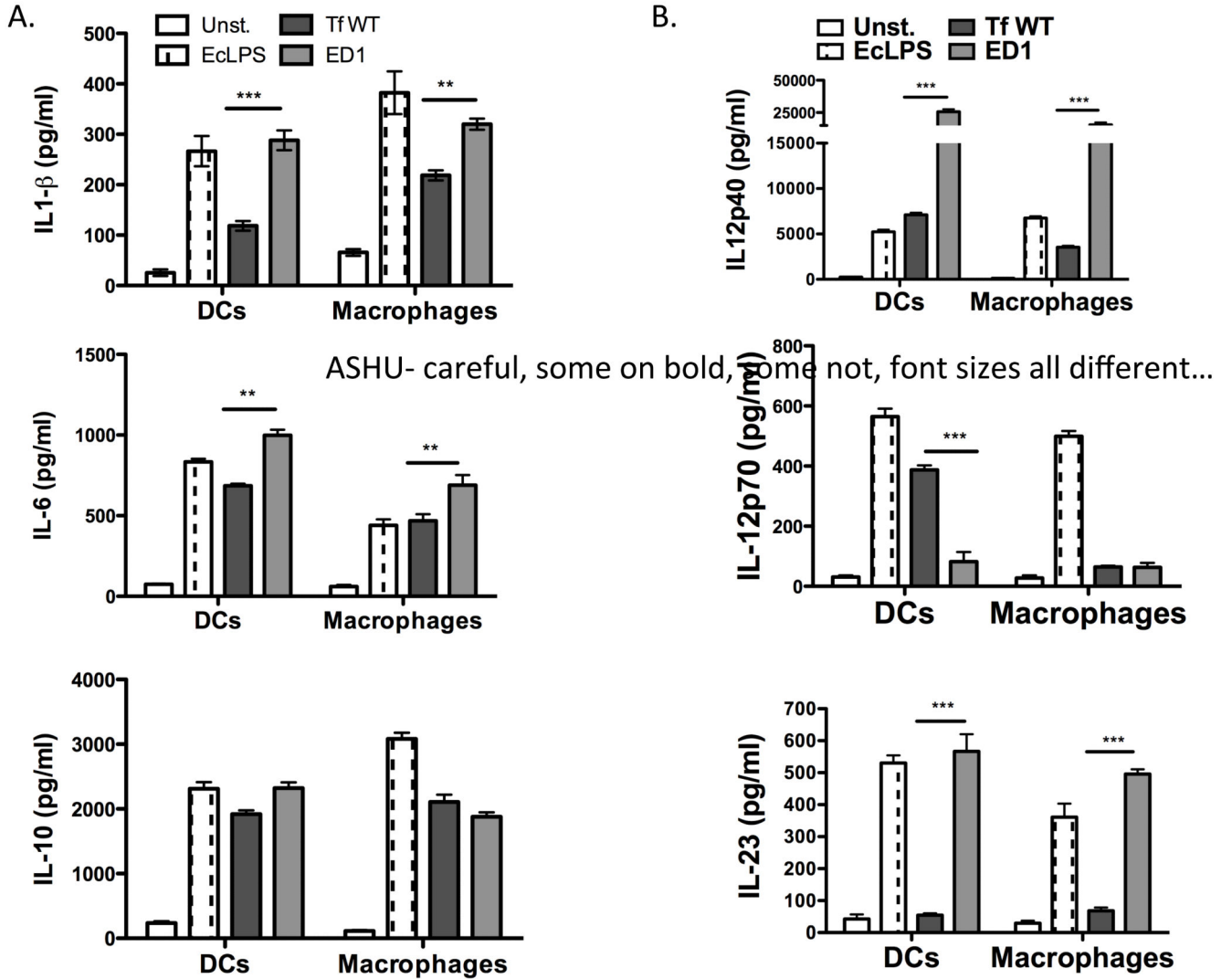
Fig. 2. *T. forsythia* surface glycosylation differentially regulates cytokine expression in macrophages and dendritic cells

Inflammatory cytokine levels (A. IL-1 β, IL-6 and IL-10; B. IL12p40, IL12p70-, IL-23) were examined by ELISA in supernatants of mouse DC's and peritoneal macrophages following challenge with either the wild-type (Tf WT) or the glycosylation deficient mutant (ED1) of *T. forsythia*. The data show the means ± standard deviations of triplicate determinations in one of 3 independent sets of experiments that yielded similar results; statistically significant differences between the groups are indicated by asterisks (***, $p<0.001$; **, $p<0.01$; *, $p< 0.05$).
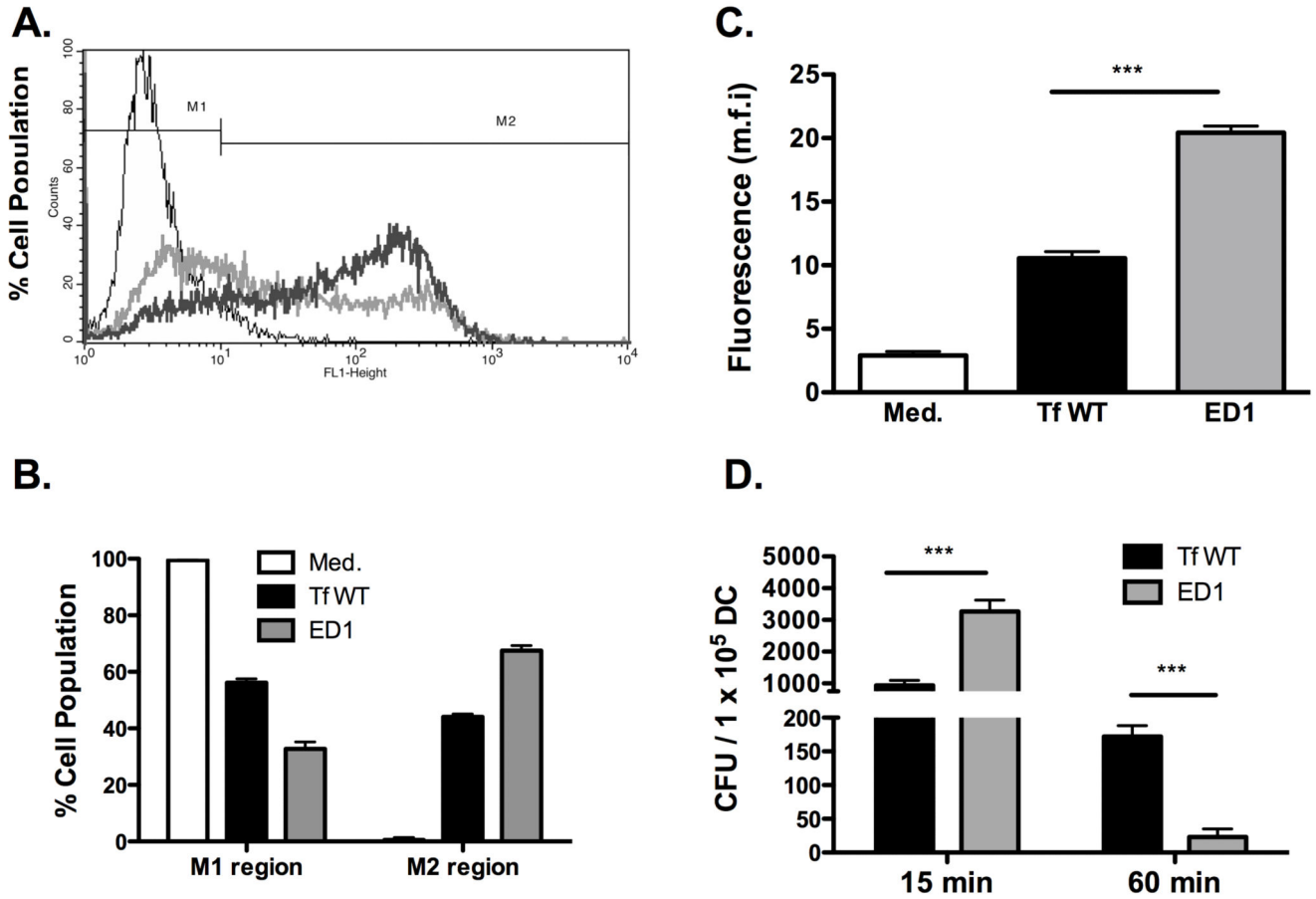
Fig. 3. Abrogation of surface glycosylation in *T. forsythia* causes enhanced dendritic cell association

Association of FITC-labeled wild-type (Tf WT) and ED1 strains was assessed by flow cytometry. (A) Representative traces of bacteria bound/engulfed by BMDCs are demarcated by the thick grey (wild-type strain) and dark (ED1 strain) lines. Autofluorescence signal is demarcated by the thin line (untreated BMDCs) and corresponds to BMDCs without bound/ ingested bacteria. (B) Bar graphs show percentages of BMDCs in gates M1 (representing the background autofluorescence and unbound bacteria) and M2 (representing brightly fluorescent cell population with bound and/or internalized FITC-labeled bacteria. (C) Bar graphs represent the mean fluorescent intensities ($\pm$S.D.). (D) Bacterial killing by DCs. Dcs were infected with bacteria (wild-type or ED1) at an MOI of 10. The number of viable bacteria were determined (CFU) at indicated time points post infection. Data represent mean CFU ($\pm$S.D.) per 10^5 DC cells of triplicate readings from two independent experiments. ***$P<0.001$.
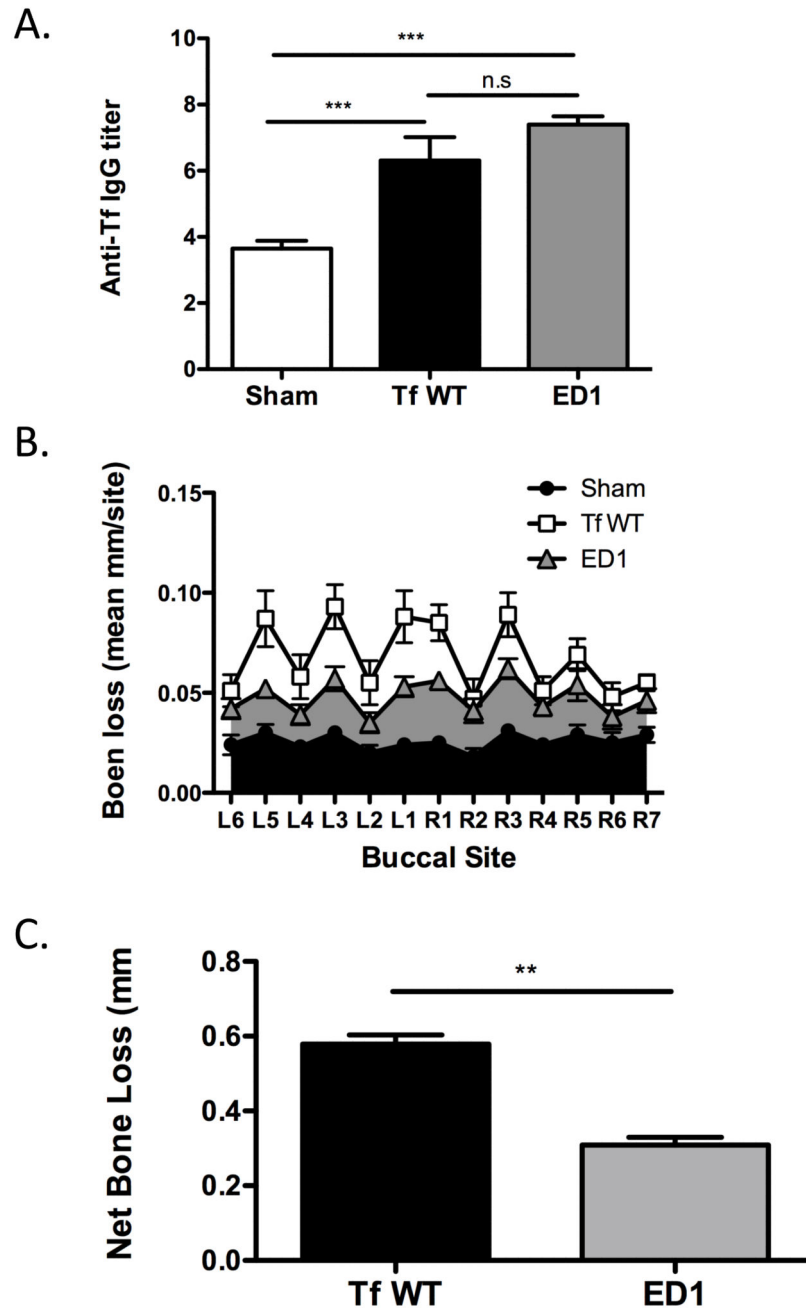
Fig. 4. ***T. forsythia* wild-type strain is more virulent than the glycosylation deficient ED1 mutant strain in a mouse model of periodontitis**

(A) Specific and cross-reactive antibodies are elevated in mice following oral infection. Sera from mice after 6 weeks of first infection (sham, Tf WT, or ED1) were analyzed for *T. forsythia* specific IgG by ELISA. Antibody levels are presented as $\log_2$ titers. Data represents means and standard deviations for each group (n=8), and statistical differences between the group means was determined (*, $p<0.05$ vs sham-infected group; #, $p<0.05$ vs Tf infected group). (B & C) ED1 mutant causes significantly less bone loss compared to the wild-type strain. Mice (n = 8) were infected by oral gavage with 6 doses (10^9 cells/dose) of

either *T. forsythia* wild-type strain (10^9 cells/dose; Tf WT) or *T. forsythia* ED1 mutant or sham-infected. (B) Alveolar bone destruction was assessed after 6 weeks by measuring the distance from the ABC to the CEJ at 14 maxillary buccal sites per mouse (R1-R7 = right jaw; L1-L7 = left jaw). (C) Net bone loss induced by wild-type or ED1 bacteria was calculated as mean total ABC-CEJ distance of bacterially infected group minus mean total ABC-CEJ distance of the sham-infected group. The data show that the net bone loss caused by the wild-type strain is significantly higher than that by the ED1 mutant. Bars indicate means and standard deviations. Data were analyzed by a Mann-Whitney unpaired *t* test, and statistically significant differences are indicated with an asterisk (***, *p*<0.001; **, *p*<0.01; n. s. not significant).
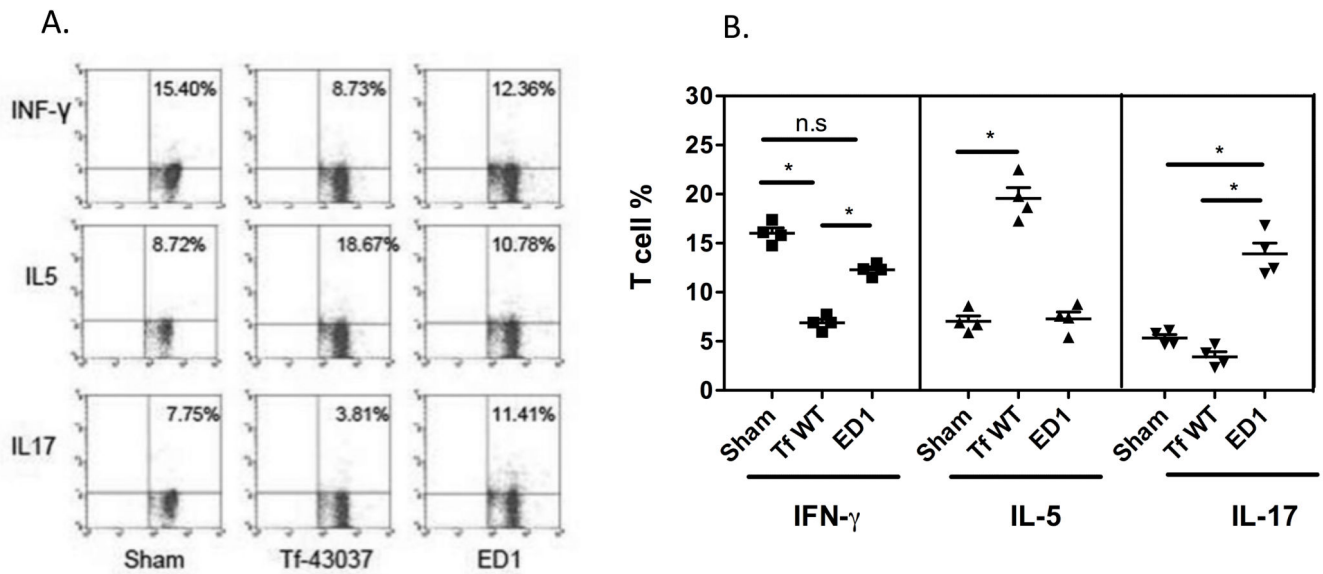
Fig. 5. *T. forsythia* glycosylation deficient ED1 mutant induces Th17 cells following infection
Production of IFN-γ, IL-5 and IL-17 in cervical lymph nodes of mice. Mice (n=4) were
infected 3 times at 48 h intervals. 72 h after the final infection, cLN cells were stimulated
with anti-CD3 and anti-CD28 Abs for 48 h. Cells were then stimulated with ionomycin and
PMA for 4-6 h prior to intracellular staining for IL-5, IFN-γ or IL-17 (A) Representative
flow cytometry dot plots of CD4^{+} T cells from sham and bacteria infected mice
intracellularly stained for IL-5, IFN-γ or IL-17. (B) Bar graphs showing percentages (mean
and standard deviations) of specific cytokine positive T cells for each group. Statistically
significant differences between the groups is indicated by; *, *p*< 0.05, n.s, not significant.
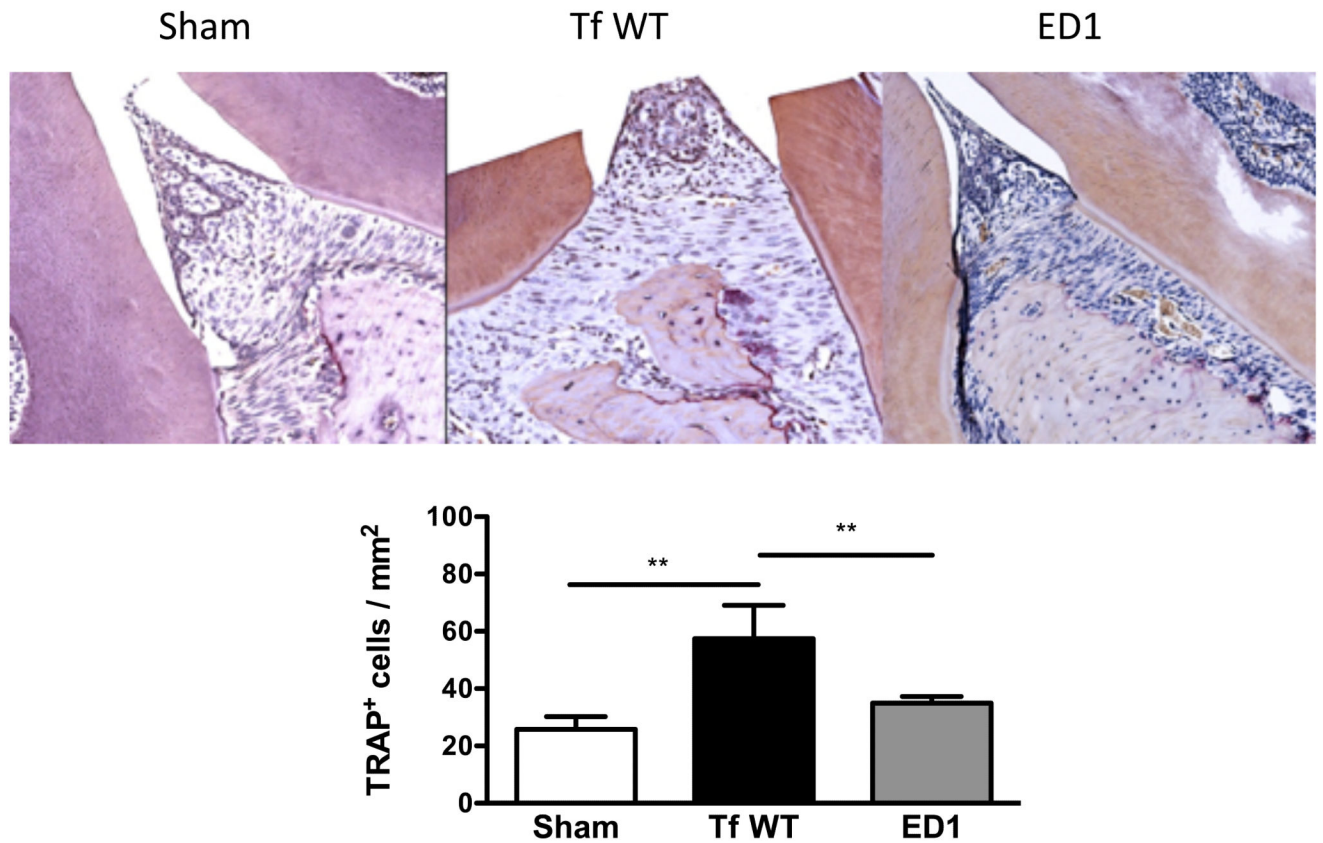
Fig. 6. *T. forsythia* wild-type strain induces increased osteoclastic activity in alveolar bone
(A) Representative histological sections showing TRAP^{+} cells from sham- and bacteria-infected mice. (B) Average number of TRAP^{+} cells in 10 high power magnification fields/ slide (4 mice/group). Statistically significant differences between groups is indicated by; **, *p*<0.01.
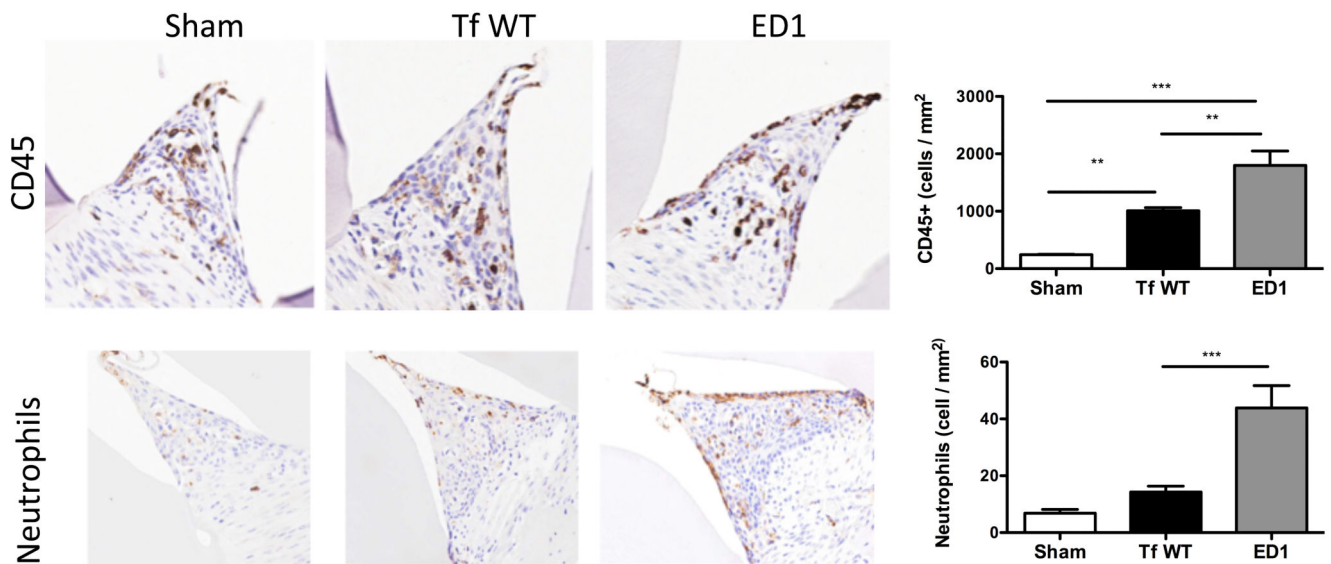
Fig. 7. *T. forsythia* glycosylation deficient ED1 mutant induces enhanced lymphocytes/neutrophil infiltration following infection

(A) Immunohistochemical staining for total inflammatory cells (CD45 positive) and neutrophils in gingival tissue 3 weeks following infection. All images are representative of 400x magnification. (B) Slide images were viewed with Aperio Image Scope viewing software and the inter-dental areas from the first to third molar were used to quantify inflammatory cells. Bar graphs showing number of CD45 positive and neutrophil antibody positive cells. Statistically significant differences between the respective *T. forsythia*-infected and sham-infected groups is indicated by; ***, $p<0.001$; **, $p<0.01$; *, $p< 0.05$, n.s, not significant.
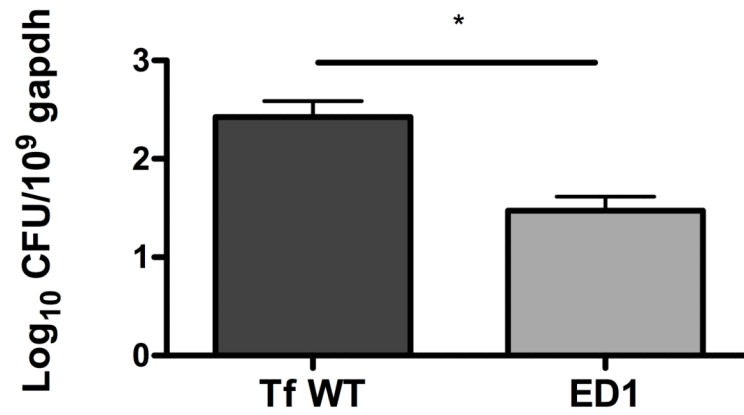
Fig. 8. Glycosylation deficiency impairs bacterial survival
Bacterial loads in gingival tissues from mice infected mice with *T. forsythia* wild-type or ED1 strains on day 10 postinfection as determined by quantitative real-time PCR. The bars and error bars indicate the means and standard deviations for four mice in each group; *, $p < 0.05$.
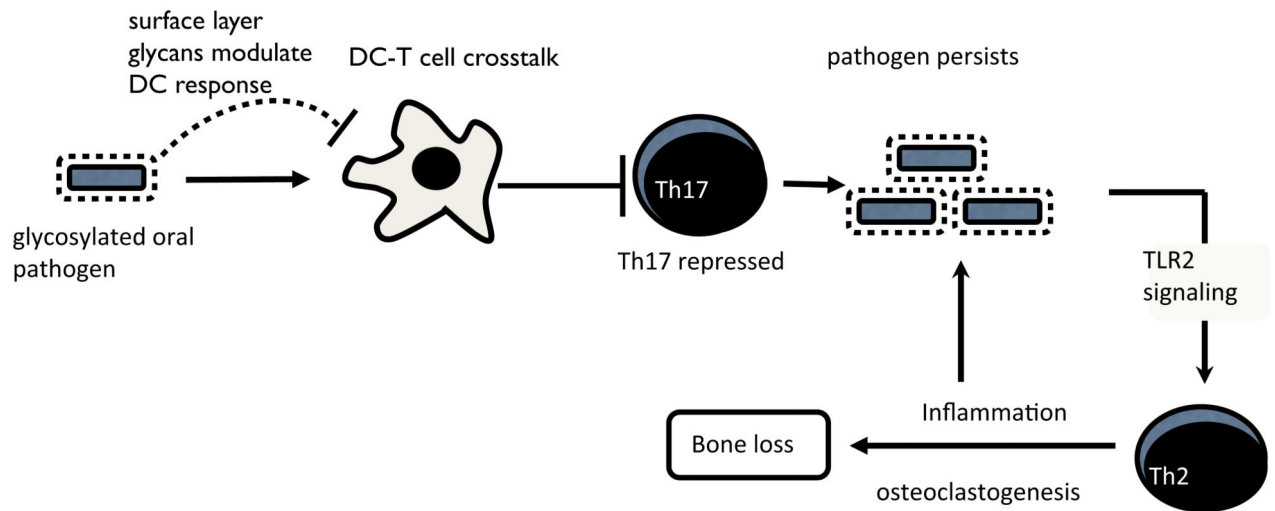
Fig. 9. A model depicting the role of *T. forsythia* surface glycosylation in pathogenesis
The S-layer glycoproteins modulate DC effector functions to suppress Th17 responses, promoting bacterial persistence in the oral cavity. Bacteria then exploit TLR2 signaling to favor dominance of Th2 responses. The TLR2-Th2 inflammatory axis causes tissue destruction and drives osteoclastogenesis. Concurrently, inflammation promotes bacterial growth by making available peptides, heme and other factors as nutrients.